Design, Modeling, and Control of a Brushless Permanent Magnet Motor for Electric Vehicles

Mohamed Arbi Khlifi
Department of Electrical Engineering, Islamic University of Madinah, Saudi Arabia | University of Tunis, ENSIT, Labo SIME, Tunisia
medarbi.khlifi@gmail.com (corresponding author)

Marwa Ben Slimene
College of Computer Science and Engineering, University of Ha'il, Saudi Arabia | University of Tunis, ENSIT, Labo SIME, Tunisia
benslimene.marwa@gmail.com

Received: 7 November 2023 | Revised: 18 November 2023 | Accepted: 20 November 2023

 DOI: https://doi.org/10.48084/etasr.6600

ABSTRACT

Electric Vehicles (EVs) are becoming more and more common. In addition to their ecological advantages, EVs have demonstrated their efficiency in curtailing travel expenses by transitioning from gasoline to electricity, which is significantly less costly. This study proposes a Brushless Permanent Magnet Motor (BPMM) design for EVs, models the influence of average and ripple torque, and evaluates its efficiency compared to other designs. The validity of the proposed design was supported by simulation results.

Keywords-brushless permanent magnet motor; electric vehicle (EV); control analysis; EV design; PI controller

I. INTRODUCTION

The problems of vehicle environmental effects and fuel consumption are getting worse as a result of the vastly expanded number of vehicles on the road. The urgent call for cars with high fuel efficiency and minimal emissions attracts significant interest from all corners of the society. Many alternative drive trains, including fuel-cell hybrid vehicles, have been proposed to address this problem [1-2]. To improve overall efficiency, the motor is either used to supplement or replace the conventional internal combustion engine. The battery provides power to the all-electric car whereas its main issue is the reasonable-sized battery limited driving range. In a hybrid electric vehicle, the battery and internal combustion engine function as a single hybrid energy source. Under two or more sources, control becomes more complex while the driving range and system efficiency increase. However, hybrid electric cars cannot fully achieve zero emissions while the internal combustion engine is present [3-4].

The growing cost of fossil fuels and their carbon emissions have been the main drivers of the mandate for renewable energy adoption. Solar and wind power are among the most popular renewable energy resources among energy suppliers and researchers [5-6]. PV and wind sources, on the other hand, are unpredictable in their operation. The power produced by PV and wind is highly dependent on solar irradiation and wind speed [7-8]. As a result, effective storage devices are used to ensure a constant power supply. Fuel cell benefits include an efficient and extraordinary power density and a flexible structure. Electric applications greatly favor the proton exchange membrane fuel cell due to its small size, high power density, and low noise emission [7-8]. Fuel cells are the best alternative for reliable power because of their low environmental impact. Their slow thermodynamic and electrochemical properties allow them to respond to transient conditions as quickly as needed [9-11]. Performance can be adjusted by controlling the interfacing devices that connect them to the electrical grid. Additionally, a single cell's voltage output is insufficient for grid connection. Many fuel cells are linked in both parallel and series configurations to provide a large DC voltage [12-14]. Unfortunately, the system cost grows and the fuel cell competence declines as the number of fuel cells expands. High-gain converters [15-17] are used to overcome this problem, transforming low voltage into high. Boost converters are characterized by their high gain and low-duty ratio. In contrast, high-duty ratio operation improves converters' otherwise poor efficiency [18-19].

To obtain a high gain in a low-duty cycle, a converter was presented in [20-21] using a linked inductor and a high-frequency grade transformer. Converters were expensive and needed consistent maintenance. Several different maximum power point tracking techniques were thoroughly discussed in [22-25]. A better optimization strategy was established in [26-28] to improve the energy extraction from fuel cell implementations. An enhanced dynamic cuckoo search algorithm was developed for practice in fuel cell solicitations, dealing with the drawbacks of the conventional approach,

which did not adjust the duty cycle depending on varying environmental temperatures. In [29-31], a new PV/fuel cell setup was designed to optimize the system linked to the grid, evaluated in three different grid load scenarios.

This study focuses on the modeling, analysis, and design approach for permanent magnetic synchronous motors used in EVs. The proposed interleaved design of the permanent magnet alternating current motor was validated in MATLAB/Simulink. The interleaved inverter ensures minimization of output current ripples as well as the system reliability.

II. MODELING THE BPMM FOR EV

SS equations are used to calculate motor voltage and current:

$$V_{qs}^{r} = r_s\, I_{qs}^{r} + w_r\, L_d I_{ds} + w_r\, \lambda_m^{'} \quad (1)$$

$$V_{ds}^{r} = r_s I_{ds}^{r} - w_r\, L_q I_{qs}^{r} \quad (2)$$

$$T_e = \frac{3}{2}\,\frac{p}{2}\,[\lambda_m I_{qs}^{r} + (L_d - L_q)\, I_{qs}^{r}\, I_{ds}^{r}] \quad (3)$$

The step input goes through a low-pass filter to control disturbances in the V_{dc} output. This low-pass filter is arbitrarily chosen. The step input goes through a current regulator block (4), which is a voltage-based current modulator:

$$v_{qs}^{r} = w_r L_d i_{ds}^{r} + w_r \lambda_m + k_q (i_{qs}^{r} - i_{qs}) \quad (4)$$

A. Current Regulator

A current regulator is an electrical circuit or device that controls the current flow in a circuit even when the supply voltage or load resistance vary. In other words, it guarantees that the current flowing through a circuit stays constant even when other elements such as the load's resistance or power supply voltage vary. The charging and discharging of an electric vehicle's battery are regulated by a control system called the battery current regulator. The battery current regulator's job is to make sure that whether the battery is being charged or discharged, the current flows within safe working parameters.

A PI controller block can be used to create the battery current regulator in Simulink, as shown in Figure 1. The Battery Management System (BMS) provides the PI controller with the difference between the required current and the measured current as input. The battery's charging and draining are then managed using the PI controller's output. The output signal is calculated by the PI controller using a Proportional (P) and Integral (I) gain. The integral gain offers a delayed reaction to minimize any steady-state faults in the output signal, whereas the proportional gain offers a direct response to the difference between the intended and measured currents.

An essential part of an EV's electrical system is the battery current regulator, which certifies that the battery is charged and discharged safely and effectively. The battery current regulator controls the current flow to the battery, preventing overcharging and overheating, which can cause damage or even battery failure. From (4) we can get:

$$I_{qs}^{r} = \frac{K_d - I_{qs}^{r}}{r_s + L_q} \quad (5)$$

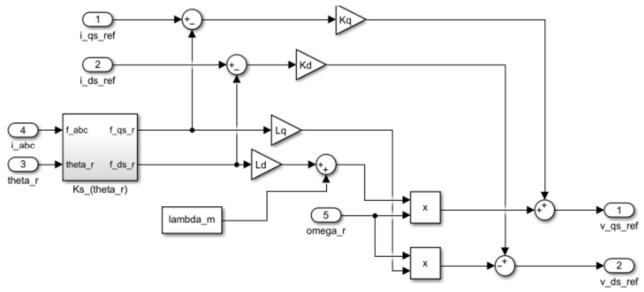

Fig. 1. PI current regulator block diagram.

B. Pulse Width Modulation (PWM)

An EV uses a current modulator, which is an electrical component to regulate the amount of current flowing from the battery to the motor. It is necessary to the powertrain system and is in charge of the vehicle's smooth functioning. Figure 2 shows the modulator block (sine triangle PWM with third harmonic injection). The intended stator voltages, the rotor position, and the DC voltage are the inputs of the modulator block. For transistors, the outputs serve as switching signals.

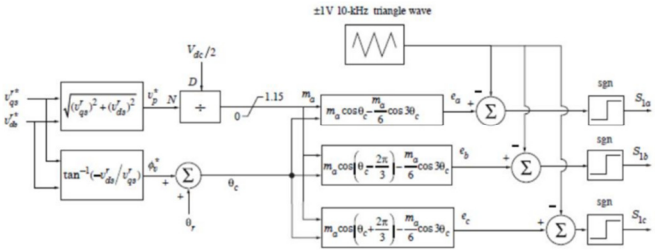

Fig. 2. Block diagram for the pulse width modulation modulator.

If the voltage increases over 1, the premise regarding PWM is nullified. Signal strengths are within ±1.5 and are separated by 120°. An electronic device, known as a motor controller, controls the speed, torque, and direction of an electric motor. Such devices are typically used to control the movement of machines and equipment in various industries, such as manufacturing, robotics, and automation. Motor control works by adjusting the power supplied to the motor. It receives signals from the control system or the operator telling the amount and direction of current to supply to the motor. The controller then adjusts the power delivered to the motor accordingly using techniques such as Pulse Width Modulation (PWM) and Direct Current (DC) control.

III. DESIGN OF A BRUSHLESS PERMANENT MAGNET MOTOR (BPMM)

ENSTROJ produces the high-performance EMRAX 208 electric motor, which can be employed in both aerospace and electric car uses. It is a Brushless Permanent Magnet Motor (BPMM) with a liquid cooling system that can run on both AC and DC power sources to provide dependable performance in challenging tasks. The motor is perfect for weight-sensitive uses, such as electric aircrafts, because it is lightweight and has a high power-to-weight ratio. This type of motor is highly productive, with a stated efficiency of over 95% in high-power settings.

The number of poles in a motor is an important parameter that affects its speed-torque and other performance characteristics. In general, a higher number of poles in a motor leads to a lower speed and higher torque output, while a lower number of poles leads to a higher speed and lower torque output.

$$p\lambda_{qs}^{r} = v_{qs}^{r} - r_s i_{qs}^{r} - w\lambda_{ds}^{r} \quad (6)$$

$$p\lambda_{ds}^{r} = v_{ds}^{r} - r_s i_{ds}^{r} - w\lambda_{qs}^{r} \quad (7)$$

$$\lambda_{ds}^{r} = L_d i_{ds}^{r} + \lambda_m \quad (8)$$

$$\lambda_{qs}^{r} = L_q i_{qs}^{r} \quad (9)$$

$$T_e = \frac{3}{2}\frac{P}{2}\left[\lambda_m i_{qs}^{r} + (L_d - L_q) i_{ds}^{r} i_{qs}^{r}\right] \quad (10)$$

The flux constant of the BPMM, also known as the back-EMF constant, depends on the specific version or variant of the motor. The standard version of the motor has a flux constant of approximately 0.0275 V/(rad/s), or equivalently, 0.00438 V/(rpm). This means that for a given rotor speed in radians per second (rad/s), the back-EMF generated by the motor is approximately 0.0275 times the speed in volts. Similarly, for a given rotor speed in revolutions per minute (rpm), the back-EMF is approximately 0.00438 times the speed in volts.

The flux constant is an important parameter that describes the relationship between the motor's electrical and mechanical characteristics. Specifically, it relates the back-EMF generated by the motor to its rotational speed and can be used to determine the motor's torque output and efficiency under different operating conditions. The standard version of the motor has a rated stator resistance of approximately 0.046 Ω at 25°C. However, this value may vary depending on the specific motor and operating conditions. The stator resistance is an important parameter that affects the motor's performance and efficiency. It determines the amount of power loss due to the resistance of the stator windings and can affect the current, torque, and speed characteristics of the motor. It is typically measured and specified at a reference temperature, such as 25°C, and may change as the motor heats up during operation.

The inductances of the BPMM on the *d*-axis and *q*-axis depend on the specific version or variant of the motor. The *d*- and *q*-axes inductances are important parameters that affect the motor's performance and control characteristics. They determine the rate of change of the magnetic field in the motor's rotor and can influence the motor's torque and speed characteristics under different operating conditions. The inductances are typically measured and specified using standard test methods, such as the three-phase short-circuit method or the two-phase open-circuit method.

IV. SIMULATION OF THE PERMANENT MAGNET MOTOR (BPMM)

Simulink is engaged to calculate and plot the maximum torque-versus-speed envelope and maximum mechanical power-versus-speed for a given drive system. The simulation was performed using MATLAB code. The code considers various parameters, such as the number of poles, flux constant, stator resistance, inductances, battery voltage, filter parameters, and current and voltage limits. The optimal BPMM was applied to the EV model to create a Simulink-based simulation model that combined the forward and backward simulation models. In another way, the driving schedule requires a certain torque and speed from the vehicle, and each module needs the required torque and speed from its superior module in the direction of the backward simulation data flow. When the data flow reaches the final energy storage, the battery will provide the required amount of energy. The simulation results are plotted, showing the maximum torque versus mechanical speed and the maximum mechanical power versus mechanical speed, as shown in the following figures.

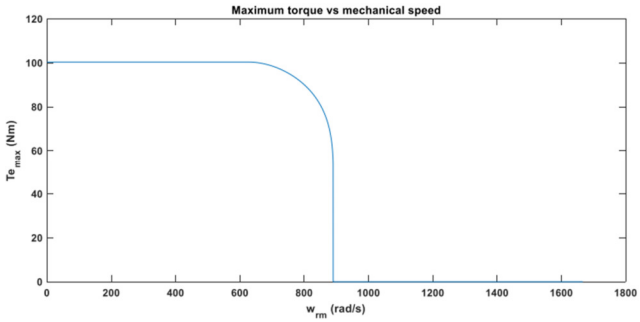

Fig. 3. Maximum torque of the BPMM.

Figure 3 illustrates the maximum torque versus mechanical speed for a specific system. Up to 700 rad/s, torque is limited by current, but beyond that, both current and voltage constraints come into play. A step change in I_{qs}^{r} was simulated while keeping the mechanical speed constant. The simulation plots the stator voltages, stator currents, DC voltage output, DC current, battery current, and electrical torque over time. Figure 4 depicts the system's response to the step change in I_{qs}^{r}, displaying the variation of DC voltage output (V_{dc}) over time from the filter block. Although it is expected to be 350 V, it fluctuates between 348V and 352V due to high-frequency harmonics in the inverter current (I_{dc}). Figure 5 shows the stator *a*-phase voltage (V_{as}) as a function of time. The peak value corresponds to approximately 2/3 of V_{dc}, which is around 233 V, as expected. The voltage values change in five distinct steps (2/3, 1/3, 0, -1/3, -2/3) of V_{dc} at the starting time. Since the BPMM acts as an EV's traction machine, performance analysis across the speed range is required. Figure 6 demonstrates the torque envelopes. The ideal machine produces more torque in the high-speed range and less torque in the low-speed range compared to the original BPMM.

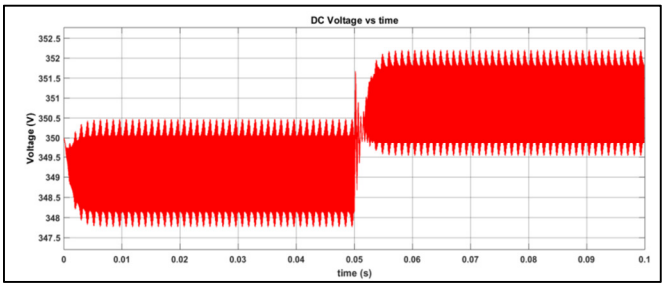

Fig. 4. Build up the DC voltage of the BPMM.

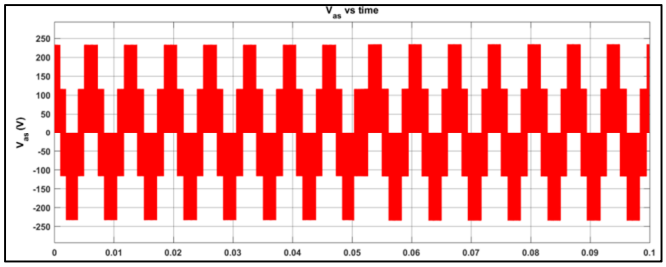

Fig. 5. Evaluation of the stator a-phase voltage (V_{as}) of the BPMM.

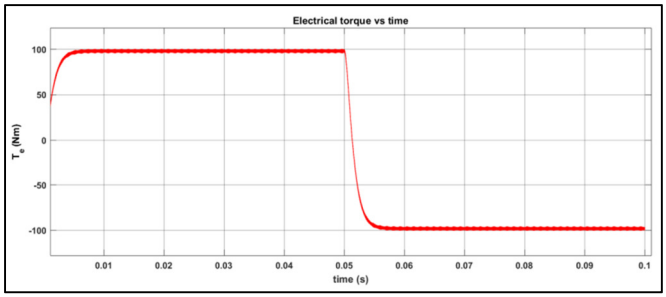

Fig. 6. Electric torque (T_e) of the BPMM.

When a step change occurs, it takes approximately 3 times the time constant ($\tau = Kq\,/\,(rs + Lq)$) for T_e to reach a steady-state value of around 100 Nm. The maximum value is approximately 210 A, but the current exhibits significant noise and fluctuates rapidly between the maximum value and zero. Figure 7 illustrates the battery current (I_{batt}) as a function of time. During positive I_{qs}^{r}, the maximum value is approximately 91 A, which closely matches the calculated value. When I_{qs}^{r} changes to negative, there is an immediate recharging cycle.

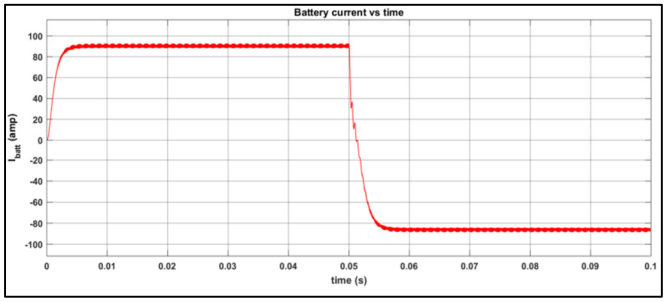

Fig. 7. Control of the battery current in the EV.

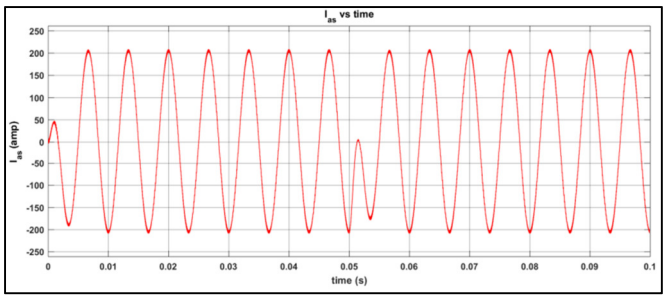

Fig. 8. Control of the battery current in the EV.

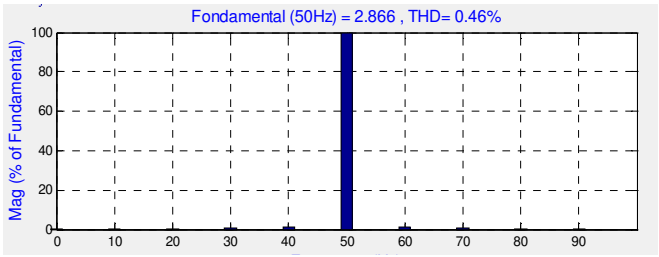

Fig. 9. Harmonic spectrum of the optimal BPMM.

Figure 8 shows the stator a-phase current (I_{as}) as a function of time. It exhibits a sinusoidal waveform with a peak amplitude of 208 A, slightly below the input value of 210 A. At 0.05 s, there is a phase shift of 180° due to a negative step. The no-load-back EMF of the ideal BPMM at a base speed of 1200 rpm is sinusoidal. The pertinent harmonic spectrum is computed in the interim. Figure 9 illustrates that the total harmonic distortion (THD) is merely 2.8%.

V. CONCLUSION

This study proposed a BPMM design, modeled, and controlled to meet the demands of various driving situations for EVs. It was shown that the proposed design approach considered the maximum operating torque and performance requirements to respond to the demands of various driving scenarios for EVs. The proposed design approach, which considers the maximum operating speed and performance requirements throughout the entire torque range, was shown to work well to produce a preliminary BPMM with good performance. The viability of using a BPMM in an EV was demonstrated by both analysis and simulation results, validating its optimization results for EV traction devices.

ACKNOWLEDGMENT

The authors extend their appreciation to the Scientific Research (DSR) at the Islamic University of Madinah for founding this research work through project number 1043.

REFERENCES

[1] D. Q. Nguyen, L. D. Hai, D. B. Minh, and V. D. Quoc, "Analysis of Electromagnetic Parameters of Hybrid Externally Excited Synchronous Motors for Electric Vehicle Applications," *Engineering, Technology & Applied Science Research*, vol. 13, no. 3, pp. 10670–10674, Jun. 2023, https://doi.org/10.48084/etasr.5824.

[2] M. Slimene, "Energy-Efficient Self-Excited Brushless DC Motor for Refrigeration Systems," *Prezglad Elektrotechniczny*, vol. 1, no. 10, pp. 75–78, Oct. 2023, https://doi.org/10.15199/48.2023.10.14.

[3] Y. Kassem, H. Gokcekus, and A. Aljatlawe, "Utilization of Solar Energy for Electric Vehicle Charging and the Energy Consumption of Residential Buildings in Northern Cyprus: A Case Study," *Engineering, Technology & Applied Science Research*, vol. 13, no. 5, pp. 11598–11607, Oct. 2023, https://doi.org/10.48084/etasr.6142.

[4] M. A. Khlifi and M. B. Slimene, "Efficiency of a Six-Phase Induction Generator Employing a Static Excitation Controller to Generate AC Power for Wind Energy," *IEEE Access*, vol. 11, pp. 28791–28799, 2023, https://doi.org/10.1109/ACCESS.2023.3260775.

[5] V. K. B. Ponnam and K. Swarnasri, "Multi-Objective Optimal Allocation of Electric Vehicle Charging Stations and Distributed Generators in Radial Distribution Systems using Metaheuristic Optimization Algorithms," *Engineering, Technology & Applied Science Research*, vol. 10, no. 3, pp. 5837–5844, Jun. 2020, https://doi.org/10.48084/etasr.3517.

[6] M. Ben Slimene and M. A. Khlifi, "Investigation on the Effects of Magnetic Saturation in Six-Phase Induction Machines with and without Cross Saturation of the Main Flux Path," *Energies*, vol. 15, no. 24, Jan. 2022, Art. no. 9412, https://doi.org/10.3390/en15249412.

[7] P. T. Giang, V. T. Ha, and V. H. Phuong, "Drive Control of a Permanent Magnet Synchronous Motor Fed by a Multi-level Inverter for Electric Vehicle Application," *Engineering, Technology & Applied Science Research*, vol. 12, no. 3, pp. 8658–8666, Jun. 2022, https://doi.org/10.48084/etasr.4935.

[8] M. A. Khlifi, "Explaining the d-q Magnetic Couplings Theoretically in Saturated Smooth Air-Gap AC Machines," *Engineering, Technology & Applied Science Research*, vol. 9, no. 1, pp. 3739–3743, Feb. 2019, https://doi.org/10.48084/etasr.2327.

[9] D. B. Minh, N. H. Phuong, V. D. Quoc, and H. B. Duc, "Electromagnetic and Thermal Analysis of Interior Permanent Magnet Motors Using Filled Slots and Hairpin Windings," *Engineering, Technology & Applied Science Research*, vol. 12, no. 1, pp. 8164–8167, Feb. 2022, https://doi.org/10.48084/etasr.4683.

[10] M. B. Slimene and M. A. Khlifi, "Performance Limits of Three-Phase Self-Excited Induction Generator (SEIG) as a Stand Alone DER," *Journal of Electrical Engineering and Technology*, vol. 12, no. 1, pp. 145–150, 2017, https://doi.org/10.5370/JEET.2017.12.1.145.

[11] A. Khadhraoui, T. Selmi, and A. Cherif, "Energy Management of a Hybrid Electric Vehicle," *Engineering, Technology & Applied Science Research*, vol. 12, no. 4, pp. 8916–8921, Aug. 2022, https://doi.org/10.48084/etasr.5058.

[12] M. Slimene, "Solar based Air Conditioner with Standalone BLDC, Charger Controller and Battery Backup for Improved Efficiency," *Prezglad Elektrotechniczny*, vol. 1, no. 9, pp. 143–146, Sep. 2023, https://doi.org/10.15199/48.2023.09.26.

[13] M. A. Khlifi and H. Rehaoulia, "General modeling of saturated AC machines for industrial drives," *COMPEL: The International Journal for Computation and Mathematics in Electrical and Electronic Engineering*, vol. 35, no. 1, pp. 44–63, Jan. 2016, https://doi.org/10.1108/COMPEL-12-2014-0346.

[14] H. Aygun and M. Aktas, "A Novel DTC Method with Efficiency Improvement of IM for EV Applications," *Engineering, Technology & Applied Science Research*, vol. 8, no. 5, pp. 3456–3462, Oct. 2018, https://doi.org/10.48084/etasr.2312.

[15] W. Li, T. W. Ching, and K. T. Chau, "Design and analysis of a new parallel-hybrid-excited linear vernier machine for oceanic wave power generation," *Applied Energy*, vol. 208, pp. 878–888, Dec. 2017, https://doi.org/10.1016/j.apenergy.2017.09.061.

[16] M. B. Slimene, M. A. Khlifi, M. B. Fredj, and H. Rehaoulia, "Modeling of a Dual Stator Induction Generator with and Without Cross Magnetic Saturation," *Journal of Magnetics*, vol. 20, no. 3, pp. 284–289, 2015, https://doi.org/10.4283/JMAG.2015.20.3.284.

[17] T. Ding, N. Takorabet, F.-M. Sargos, and X. Wang, "Design and Analysis of Different Line-Start PM Synchronous Motors for Oil-Pump Applications," *IEEE Transactions on Magnetics*, vol. 45, no. 3, pp. 1816–1819, Mar. 2009, https://doi.org/10.1109/TMAG.2009.2012772.

[18] K. Jyotheeswara Reddy and S. Natarajan, "Energy sources and multi-input DC-DC converters used in hybrid electric vehicle applications – A review," *International Journal of Hydrogen Energy*, vol. 43, no. 36, pp. 17387–17408, Sep. 2018, https://doi.org/10.1016/j.ijhydene.2018.07.076.

[19] M. Ben Slimene, M. A. Khlifi, M. Ben Fredj, and H. Rehaoulia, "Analysis of Saturated Self-Excited Dual Stator Induction Generator for Wind Energy Generation," *Journal of Circuits, Systems and Computers*, vol. 24, no. 09, Oct. 2015, Art. no. 1550129, https://doi.org/10.1142/S0218126615501297.

[20] X. Liu, K. Reddi, A. Elgowainy, H. Lohse-Busch, M. Wang, and N. Rustagi, "Comparison of well-to-wheels energy use and emissions of a hydrogen fuel cell electric vehicle relative to a conventional gasoline-powered internal combustion engine vehicle," *International Journal of Hydrogen Energy*, vol. 45, no. 1, pp. 972–983, Jan. 2020, https://doi.org/10.1016/j.ijhydene.2019.10.192.

[21] A. Wang, Y. Jia, and W. L. Soong, "Comparison of Five Topologies for an Interior Permanent-Magnet Machine for a Hybrid Electric Vehicle," *IEEE Transactions on Magnetics*, vol. 47, no. 10, pp. 3606–3609, Jul. 2011, https://doi.org/10.1109/TMAG.2011.2157097.

[22] B. S. Marwa, A. K. Mohamed, B. F. Mouldi, and R. Habib, "Effect of the stator mutual leakage reactance of dual stator induction generator," *International Journal of Electrical Energy*, vol. 2, no. 3, pp. 1810–1818, 2014.

[23] Y. Yang *et al.*, "Design and Comparison of Interior Permanent Magnet Motor Topologies for Traction Applications," *IEEE Transactions on Transportation Electrification*, vol. 3, no. 1, pp. 86–97, Mar. 2017, https://doi.org/10.1109/TTE.2016.2614972.

[24] H. Xiong *et al.*, "An energy matching method for battery electric vehicle and hydrogen fuel cell vehicle based on source energy consumption rate," *International Journal of Hydrogen Energy*, vol. 44, no. 56, pp. 29733–29742, Nov. 2019, https://doi.org/10.1016/j.ijhydene.2019.02.169.

[25] M. A. Khlifi, M. Ben Slimene, M. Ben Fredj, and H. Rhaoulia, "Performance evaluation of self-excited DSIG as a stand-alone distributed energy resources," *Electrical Engineering*, vol. 98, no. 2, pp. 159–167, Jun. 2016, https://doi.org/10.1007/s00202-015-0349-y.

[26] M. F. El-Khatib, M. N. Sabry, M. I. A. El-Sebah, and S. A. Maged, "Hardware-in-the-loop testing of simple and intelligent MPPT control algorithm for an electric vehicle charging power by photovoltaic system," *ISA Transactions*, vol. 137, pp. 656–669, Jun. 2023, https://doi.org/10.1016/j.isatra.2023.01.025.

[27] X. Liu, Q. Lin, and W. Fu, "Optimal Design of Permanent Magnet Arrangement in Synchronous Motors," *Energies*, vol. 10, no. 11, Nov. 2017, Art. no. 1700, https://doi.org/10.3390/en10111700.

[28] M. B. Sliemene and M. A. Khlifi, "Persistent Voltage Control of a Wind Turbine-Driven Isolated Multiphase Induction Machine," *Engineering, Technology & Applied Science Research*, vol. 13, no. 5, pp. 11932–11936, Oct. 2023, https://doi.org/10.48084/etasr.6330.

[29] M. Y. Veeresh, V. N. B. Reddy, and R. Kiranmayi, "Modeling and Analysis of Time Response Parameters of a PMSM-Based Electric Vehicle with PI and PID Controllers," *Engineering, Technology & Applied Science Research*, vol. 12, no. 6, pp. 9737–9741, Dec. 2022, https://doi.org/10.48084/etasr.5321.

[30] M. B. Slimene, "Buck converter topology for fuel cell hybrid vehicles.," *Przeglad Elektrotechniczny*, vol. 2023, no. 9, 2023.

[31] K. Unni and S. Thale, "Energy Consumption Analysis for the Prediction of Battery Residual Energy in Electric Vehicles," *Engineering, Technology & Applied Science Research*, vol. 13, no. 3, pp. 11011–11019, Jun. 2023, https://doi.org/10.48084/etasr.5868.